UPWARDS

Deliverable D2.2

Report on AL enhancement and turbulence model

WP	2	Atmospheric model
Task	2.4	Park and turbulence model development.

Dissemination level[1]	PU	Due delivery date	31/09/2019
Nature[2]	R	Actual delivery date	31/03/2020

Lead beneficiary	SINTEF
Contributing beneficiaries	AWS Truepower

Document Version	Date	Author	Comments[3]
1.0	13.03.2020	Balram Panjwani	Draft version
2.0	31.03.2020	Balram Panjwani	Updated version

---

[1] Dissemination level: **PU** = Public. **PP** = Restricted to other programme participants (including the JU). **RE** = Restricted to a group specified by the consortium (including the JU). **CO** = Confidential. only for members of the consortium (including the JU)

[2] Nature of the deliverable: **R** = Report. **P** = Prototype. **D** = Demonstrator. **O** = Other

[3] Creation. modification. final version for evaluation. revised version following evaluation. final

Deliverable abstract

Description of task 2.3: LES-Park will be developed in OpenFoam. The wind flow in the wind park will be estimated using large eddy simulation technique (LES) technique, while the influence of the blades on the flow field will be approximated by the Actuator Line Model (ALM). Existing ALM will be improved to account for the nacelle and tower effects. A filter-based model will be designed to overcome shortcoming associated with existing turbulence model. In filter-based model, transport equations for sub filter energy and sub filter dissipation rate will be modelled and for turbulent eddy viscosity exponential relaxation function will be solved. The dissipation model based on macroscopic turbulent length scale will be implemented. The model equations will be solved in OpenFoam architecture. UPWARDS LES-Park model will be based on improved ALM and filter-based turbulence model. The LES-Park will be verified against field data for Offshore wind Park (i.e. Lillgrund).

A full CFD method (resolving wind turbines on the grid scales), methods are computationally demanding and almost impossible to apply in the design and optimization of wind farms and park control. To overcome these challenges, a method based on combing CFD and BEM has been developed [1–4]. In this coupled method, the wind turbines are not resolved on the grid, but the effect of turbines on the flow field is modelled and this effect is modelled either using the actuator disk method (ADM) or actuator line method (ALM). However, both ALM and ADM are unable to resolve the detailed geometrical features of turbine blades on a mesh. To alleviate this problem an improved ALM approach, Actuator Surface Models (ASM) for turbine blades, which take into account more geometrical details have been studied. In the present study, the ASM approach has been implemented in OpenFom. The effect of tower and nacelle is also included in the wind farm simulations. The loads on each surface of the turbine are estimated using the Blade Element Method (BEM). The model is validated with available literature data and preliminary results are presented here. Filter-based turbulence model developed by SINTEF have been implemented and tested. The work have been already presented at Deepwind conference at Trondheim Norway.

Deliverable Review

	Reviewer #1:			Reviewer #2:		
	Answer	Comments	Type*	Answer	Comments	Type*
1. Is the deliverable in accordance with						
(i) The Description of Work?	☒ Yes ☐ No		☐ M ☐ m ☐ a	☒ Yes ☐ No		☐ M ☐ m ☐ a
(ii) The international State of the Art?	☐ Yes ☐ No	*Not applicable for this deliverable*	☐ M ☐ m ☐ a	☐ Yes ☐ No	*Not applicable for this deliverable*	☐ M ☐ m ☐ a
2. Is the quality of the deliverable in a status						
(i) That allows it to be sent to European Commission?	☒ Yes ☐ No		☐ M ☐ m ☐ a	☒ Yes ☐ No		☐ M ☐ m ☐ a
(ii) That needs improvement of the writing by the originator of the deliverable?	☐ Yes ☒ No		☐ M ☐ m ☐ a	☐ Yes ☒ No		☐ M ☐ m ☐ a
(iii) That needs further work by the Partners responsible for the deliverable?	☐ Yes ☒ No		☐ M ☐ m ☐ a	☐ Yes ☒ No		☐ M ☐ m ☐ a

* Type of comments: M = Major comment; m = minor comment; a = advice

Table of content

1. Introduction

European commission target to reach carbon-neutral society by 2050 requires tremendous efforts. The electricity production from renewable is one of the best alternatives to reach that target. Offshore wind energy is one the fastest growing source of renewable electricity generation in Europe and according to the International Energy Agency (IEA), the offshore wind could become the number one source of power generation in Europe by 2040. This represents many jobs creation by the global wind industry. However, a number of economic, technical, social and environmental aspects inhibit the development of wind parks. In some cases, the costs of wind turbines may be prohibitive and the design of large wind turbines needs to be optimized in terms of material use and reliability, while in other cases the siting of wind turbines may interfere with environmental functions, such as landscape preservation. Improved predictive tools are very important for park-layout optimization and the power produced by a wind turbine placed inside an offshore wind park among other parameters depends on the approaching wind. However, the wind approaching on the downstream turbines is influenced by the neighbouring turbines. If the downstream turbine is in the shadow of other wind turbine then the approaching wind on the downstream wind turbine will be with reduced wind speed and increased turbulence. The reduced wind speed with increased turbulence affects the wake propagation of source turbine which affects the power and the loading of the target wind turbine.

The wake is classified into two categories near wake and far wake. The near wake is the area just behind the turbine rotor which is approximately up to one to three rotor diameters downstream. The near wake region, dominated by intense turbulence, mainly depends on a type of turbine, number of blades, aerodynamic shape of the blades and dimensions of turbine blades. The far wake region is a region beyond the near wake. The near wake research is very turbine specific, while the far wake research is focused on the mutual interactions of turbines and atmospherics flows, when the turbines are placed in clusters, like wind farms [3]. The far wake influences the turbine performance including power output and turbine loading. Therefore, the main attention should be focused on far wake models, wake-wake interference, turbulence models etc. [1;2]. The wakes studies have been a topic of intensive research, both experimentally and numerically during the last decades and have been reviewed by Vermeer et al. [5].

The explicit models based on a self-similar velocity profile [6–12] provide the closed form solution of the wake width and wake deficit and these models primarily used for the power prediction of turbines with reasonably accuracy. These models are computationally inexpensive while maintaining sufficient accuracy and therefore these models are preferred in industrial applications. However, these simple wake models have some shortcomings such as they are unable to account for wake-wake interaction resulting from multiple wind turbines in a park. In addition to this, these models also require wind park dependent tuning of parameters. The other wake models are called field model where flow equations are solved for estimating the flow over a wind farm.

The rapid increase in high performance computing have accelerate the use of advanced model based on elliptic field /full CFD in which an NS equation are solved on the grid and the turbines are modeled as a sink term in momentum equation. The wind turbines are modelled either using actuator disk (AD) [13–17] or actuator line (AL) [18] approach. The AD approach assumes turbine rotor as a porous medium, and AL approach resolves each blade of the turbine as a line or surface. In AL the turbine blades are represented by lines upon which a distribution of forces acts as a function of local incoming flow and blade geometry [1;2]. A main advantage of actuator line model is the representing of the blades by its airfoil data that it makes the approach well suited for wake studies [10]. The rotational effect of blades, finite blade number effect and the effect of non-uniform force distribution in the azimuthal direction are well incorporated in ALM. However, most of the AL model employed 2-dimensional drag and lift coefficients without considering the rotational effects and these lift and drag coefficient need to be corrected for the three-dimensional rotational effects as those proposed in [14]. In addition to this, there are two major limitations of the standard actuator line model: i) The

lack of an effective nacelle model. Many previous studies indicated that nacelle induced coherent structures, as nacelle act as a bluff body, have a significant impact on turbine velocity deficit in the near wake and also on wake meandering in the far wake. The ALM without a nacelle model unable to accurately capture the wake meandering of turbine, and underpredicts the apparent turbulence intensity at far wake locations. ii) A finer mesh cannot resolve more geometrical features of the turbine blade. The results of Yang et al. [1] showed that grid-independent results cannot be obtained when the mesh is refined in the actuator line model simulations. This is because more physics cannot be resolved on a finer grid in the state-of-the-art actuator type models. The accuracy of the computed results mainly depends on the parameterizations employed in actuator line models.

To overcome some of the ALM challenges, an improved ALM method so called Actuator Surface Models (ASM) will be developed in OpenFoam framework. Many versions of ASM have been developed [1–4]. Yang and Sotiropoulos [1] have developed a new class of actuator surface models for turbine blade and nacelle to take into account nacelle geometry and the geometrical effect of turbine blade. In the actuator surface model for blade, the forces are still computed using the blade element method but are distributed on the surface formed by the foil chords at different radial locations. In the actuator surface model for nacelle, the forces are distributed from the actual nacelle surface with the normal force component computed in the same way as in the direct forcing immersed boundary method and the tangential force component computed using a friction coefficient and a reference velocity of the incoming flow. Linton et al. [2] developed a new class of ASM by introducing a new rotor wake model to improve the prediction of the effective angle of attack along the span and thus the prediction of the loading distribution. This wake model is designed to be applied in varied operating conditions and environments, leading to a more realistic formation of the wake in the CFD solution and improved prediction of the response of the rotor to an unsteady flow-field. Kim et al. [3] suggested a new ASM based on the lifting line theory to eliminate the unexpected induced velocity due to the circulation, as well as to estimate the span-wise and chord-wise variation of the circulation of the blade. In addition, the method developed overcomes the need for tip-loss correction. A fixed wing case was used to validate the proposed method according to the reference line position and the number of chord-wise panels. In the next chapter, ASM implementation along with theoretical background is presented.

2. ASM implementation in UPWARDS project

The approach presented by Yang and Sotiropoulos [1] have been implemented. This methodology can simulate the flow around the turbine, including the near and the far wake. The methods developed for modelling the wind turbine based on the actuator surface concept are capable of estimating the near wake dynamics in much more details than the actuator line or actuator disk methods. These methods are derived from Blade element approaches and it can be used with any flow solvers such as CFD, potential flow, viscous/inviscid flow etc. In the current modelling approach CFD is chosen since it can resolve the flow in much greater details than any other flow solvers. To ensure the software are available for public release the ASM method is integrated in OpenFoam architecture and unsteady PisoFoam solver is updated to model wind turbines. The new solver in UPWARDS project is referred as a UPWARDS.ASM. The solver is capable of predicting the power of independent wind turbine as well as cluster of wind turbines. The turbines are modelled as a sink term in momentum equation and this is described by following generalized N-S equation.

$$\frac{\partial \rho \bar{u}_i}{\partial t} + \frac{\partial \rho \, \bar{u}_i \bar{u}_j}{\partial x_j} = -\frac{\partial \bar{p}_i}{\partial x_i} + \frac{\partial \tau_i}{\partial x_j} + \boldsymbol{S} \qquad \text{Equation 1}$$

Where ρ is the density, u is the flow velocity, $\boldsymbol{\tau}$ is the shear stress, x_i, x_j are the directions, and p is the pressure. The source term (S) in the momentum equation can be estimated either by ADM, ALM or ASM. Here in the present report, ASM approach is utilized. The nacelle and tower models are also included.

In ASM method, the point blade forces estimated on blade surface will be transferred on the background volume flow. The forces acting on the blade depends on the airfoil shapes, local angle of attack, approaching wind velocities. The concept is mainly driven from Blade Element method (BEM) commonly used in aeroelastic simulation of the wind turbines. A coupling between blade element method and CFD was proposed by Sørensen and Shen's [1;2]. In ASM as mentioned each blade is assumed as a surface and the forces acting on the surface are estimated using BEM approach. **Feil! Fant ikke referansekilden.** shows the geometrical representation of the wind turbine and their blades surface and the blade geometry is represented by a surface formed by the chord lines at different radial locations of a blade. The approaching flow introduces local forces (Lift and Drag) depending on the relative velocity, twist angle of the blade, the blade chord and local angle of attack. In ASM, the blade is represented as a surface and the blade forces are projected on a surface. A blade profiles section A-A' is plotted in **Feil! Fant ikke referansekilden.**. The fluid velocity relative to the blade, $V_{rel} = V_n e_n + (V_t - \Omega r) e_t$ decomposed into a normal component V_n and a tangential component V_t

The average local blade velocities over the blade surface is estimate using following expression

$$V_n = \frac{1}{c} \int_c u(X).e_n ds \qquad\qquad \text{Equation 2}$$

$$V_t = \frac{1}{c} \int_c u(X).e_t ds \qquad\qquad \text{Equation 3}$$

$$u(X) = \sum_{x \in gx} u(x)\delta_h(x-X)V(x) \qquad\qquad \text{Equation 4}$$

Where X are the grid point coordinates on the blade surface. Generally, the grid points on the actuator surfaces do not coincide with any background nodes. A smoothed discrete delta function (i.e. the smoothed four-point cosine function) proposed by Yang et al. [24] is employed to interpolate u (X) from the values on the background grid

$$\delta_h(x-X) = \frac{1}{V}\phi\left(\frac{x-X}{h_x}\right)\phi\left(\frac{y-Y}{h_x}\right)\phi\left(\frac{z-Z}{h_x}\right) \qquad\qquad \text{Equation 5}$$

Where x are the coordinates of the background CFD mesh, gx is the set of background grid cells, V is the volume of CFD mesh cell, δ_h is the discrete delta function.

$\phi(r)$ is the smoothed four-point cosine function [24], which is expressed as

$$\phi(r) = \begin{cases} \frac{1}{4} + \sin\left(\frac{\pi(2|r|+1)}{2}\right) - \sin\left(\frac{\pi(2|r|+1)}{2}\right) & |r| \leq 1.5 \\[2mm] \frac{5}{8} - \frac{|r|}{4} - \sin\left(\frac{\pi(2|r|+1)}{4}\right) & 1.5 \leq |r| \leq 2.5 \\[2mm] 0 & 2.5 \leq |r| \end{cases} \qquad \text{Equation 6}$$
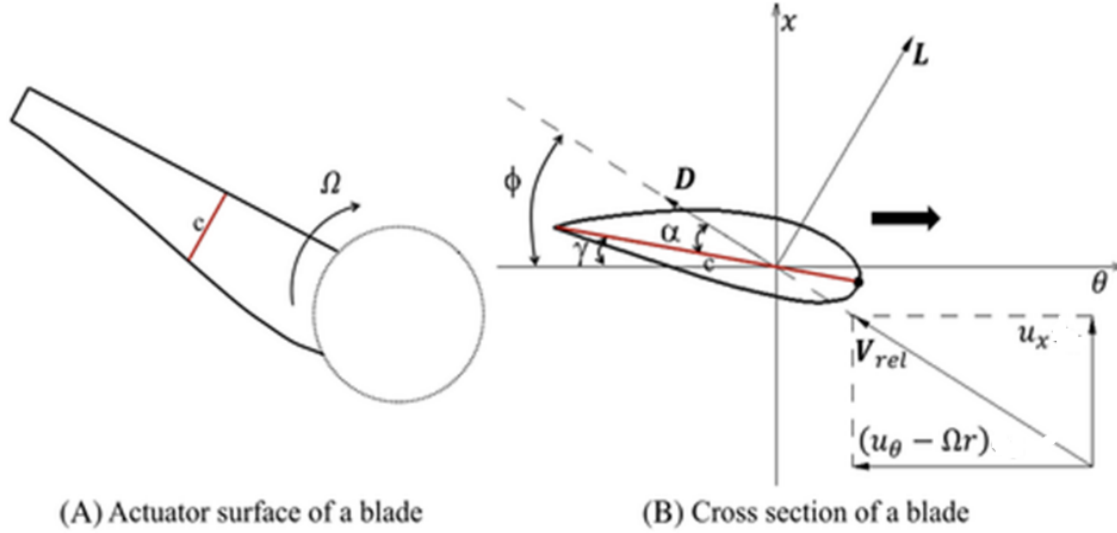
r is distance between grid points on the blade and background volume meshes. $\phi(r)$ function was employed for transferring the velocities from the background mesh onto the velocities on the blade surface and these velocities are referred here as blade velocities. These blade velocities are used in calculating the local angle of attack on the blade surface using following expression which depends on the normal blade velocity (U_n) and tangential blade velocity U_t and β which is the angle including the blade twist and the blade pitch.

$$\alpha = \tan^{-1}\left(\frac{V_n}{(V_t - \Omega r)}\right) - \beta \qquad\qquad \text{Equation 7}$$

Based on the local angle of attack and relative velocity the lift (L) and drag (D) forces per unit span are calculated.

$$L = \frac{1}{2} C_L(\alpha) \rho V_{rel}^2 C$$
Equation 8

$$D = \frac{1}{2} C_D(\alpha) \rho V_{rel}^2 C$$
Equation 9

(A) Actuator surface of a blade   (B) Cross section of a blade

Figure 1 Schematic representation of a wind turbine and approaching velocity and cross sectional view of the blade airfoil [11;12;16]

The lift and drag forces calculated on the blade surfaces are used in calculating the forces on the blades. Both lift and drag forces are transferred onto the volume mesh using following expression

$$f(x) = -\sum_{X \in g_X} f(X) \delta_h(x - X) A(X)$$
Equation 10

Where $C_l(\alpha)$ and $C_D(\alpha)$ are the lift and drag forces respectively, ρ density of the air, c is the chord length of the blade. g_X is the set of the actuator surface grid cells and A is the area of the actuator surface grid cell. The same discrete delta function as in Equation is employed. It is noted the negative sign is because that $f(x)$ represents the volume forces acting on the flow, while $f(X)$ denotes the actuator surface forces

3. Actuator surface model for nacelle

Assuming the wind turbine nacelle is cylindrical body and the frontal cross section is circular, a method proposed by Aitken et al.[19], Churchfield[20], and Wu and Porte-Agel.,[21] is implemented in OpenFoam. The nacelle is discretized into actuator lines and the velocity is sampled at one location upstream of the nacelle. A value of drag coefficient of nacelle is specified by the user and for this drag coefficient and velocities at upstream location, the drag of the nacelle is computed. The drag is divided proportionally between each actuator elements. The lift force due to nacelle is neglected. The drag force acting on each actuator element is then projected to the flow field using the similar transfer function described in the previous section.

4. Very large eddy simulation (VLES) turbulence model

Reynolds Averaged Simulations are still preferred over large eddy simulations for modelling the industrial turbulent flows due to lower computational demands. As we know LES requires finer meshes and hence larger computational resources compare to the RANS. Modelling of wind parks requires a domain size of few kilometres and grid size of many millions. Wind park modelling with LES is possible, but it is computationally demanding and therefore for industrial application RANS is a preferred choice. However, one of the challenges of using RANS approach is a selection of an appropriate turbulence model that can estimate reliable turbulence

production and dissipation in wind park simulations. The most preferred turbulence models are two equation turbulence model such as the standard k – ε model and the.

The standard k – ε model is suitable for free shear fully turbulent flows such as wind park simulations but unable to account for adverse pressure gradients [22]. On the other hand, standard k – ω model is suitable for flows where adverse pressure gradients dominate. Previous studies [23] have shown that two equation turbulence models fail to predict the velocity and turbulence quantities in the near or the far wake regions of the wind turbine and they proposed a remedy to this problem by adding a source term in the region of the turbine in the equation for the eddy dissipation of the standard two equation model. In addition, the turbulence dissipation also depends on the grid size and to overcome these challenges, Johansen et al. [24] proposed a grid independent turbulence model. In the proposed work, existing k-epsilon model is modified to account for the grid variation and a model developed by Johansen et al. [24] is implemented. The model developed by Johansen et al. [24] applies a top-hat filter to the momentum equations to filter the turbulent structures with the physical extent above a given filter size. The turbulence scales below the filter size hereafter referred as "sub filter turbulence" is accounted for by solving the transport equations for the turbulent kinetic energy and dissipation. The turbulent stresses due to the sub filter flow are modelled similar to a RANS. But, the turbulence stresses, in addition to turbulent kinetic energy and dissipation, depends on the filter length scale. In this way, the model dynamically resolves the larger flow structures responsible for mixing, dispersion and momentum exchange. One major advantage with this approach, compared to standard RANS modelling, is that gravity effects due to density gradients (buoyancy, thermal or compositional stratification) is well represented by the resolved model and thereby makes the model less vulnerable to the accuracy of closures for these specific effects [25]. The sub-filter stresses are constructed directly by using the filter size and the conventional turbulence closure. The filter is decoupled from the grid, making it possible to obtain grid independent solutions with a fixed filter scale. The turbulence model is known as a VLES (very large eddy scale) model and has later been adopted by others, e.g. Labois and Lakehal [26], Olsen et al.[25], and Panjwani and Olsen [27] The model has been validated against experiments on e.g. vortex shedding behind cylinders [24], flow across a tube bundle[26], large scale particle plumes[25], and dust flow distribution inside the room [27]. Here is a brief description of the model,

Sub filter turbulence fluctuations $u_\Delta^{'}$ are given by [24,25]

$$u_\Delta^{'} = \pi^{-1/3} \, C_K^{1/2} \, \acute{U}_\Delta^{1/3} \Delta^{1/3} \qquad \text{Equation 11}$$

Where, Δ is filter size, $\acute{U}_\Delta$ is sub filter turbulence dissipation, C_K is model constant. The sub filter turbulence viscosity depends on the length and velocity scale and it is given by the following equation

$$\nu_t = u_\Delta^{'} \cdot l_t \qquad \text{Equation 12}$$

where l_t is the turbulent length scale, and by acknowledging that the largest effective length scale is limited by the effective length scale of the sub-filter model. For a $k - \acute{U}$ model the length scale is l_{eff}

$$l_{\text{eff}} = C_\mu^{\frac{3}{4}} k^{3/2} \acute{U}^{1} \qquad \text{Equation 13}$$

with C_μ = 0.09 for the standard $k - \acute{U}$ model [28]. Combining equations (12) and (13) lead to the following expression for the kinematic turbulent viscosity

$$\nu_t = C_\mu \, \frac{k_\Delta^2}{\Delta} \, \cdot \text{MIN} \left[1 \, ; \, C \, \frac{\Delta_\Delta}{k_\Delta^{3/2}} \right] \qquad \text{Equation 14}$$

A major difference between the standard $k - \acute{U}$ model and VLES model is viscosity estimation. In $k - \acute{U}$ model, the viscosity does not depend on the grid size but the VLES model accounts for grid size which makes suitable for obtaining the grid independent results. The turbulent viscosity is given by the sub-filter model if the filter size is larger the turbulent scale based on the standard $k - \acute{U}$ model. In order to apply the VLES model in OpenFoam modelling framework an expression for the sub filter eddy time scale is required τ_{e_Δ}, which depends on the eddy viscosity and sub filter turbulence fluctuation.

$$\tau_{e_\Delta} = \frac{u_\Delta^{'\,2}}{\nu_t}$$

Equation 15

By combining Equations (14}) and (15}) we can express the sub filter eddy time scale by

$$\tau_{e_\Delta} = \frac{3}{2}\frac{\nu_t}{k_\Delta} = \frac{3}{2}C_\mu \frac{k_\Delta}{\Delta}\cdot MIN\left[1\,;C\frac{\Delta_\Delta}{k_\Delta^{3/2}}\right]$$

Equation 16

The subindex Δ in the above equation indicates that both the kinetic energy and dissipation is based on the turbulent energy residing within the length scales of the filter. More details and full derivation of the VLES model is provided by Johansen and shyy [24] . A further extension was done by Olsen et.al. [25]. The subgrid scale turbulence needs to be modelled similar to the LES model. However, the subgrid model is based on the $k-\acute{U}$ model which allows for coarser grids than the traditional LES models. In the VLES model, the turbulent viscosity becomes

$$\mu_t = \rho C_\mu \frac{k^2}{\varepsilon} MIN\left[1\,;\frac{C\Delta_\varepsilon}{k^{3/2}}\right]$$

Equation 17

Turbulence model implementation

A new turbulence model VLES has been implemented in OpenFoam, the new turbulence model is an extension of existing $k-\acute{U}$. The details of the implementation can be found in OpenFoam software

5. Implementation in OpenFoam

A code UPWARDS.ASM extended from PisoFoam is developed. This is achieved by adding a sink term in momentum equation. The momentum sink term is based on the SOWFA code [11;12] philosophy and the SOWFA code has been simplified to include actuator surface model. Equation **Feil! Fant ikke referansekilden.** shows the OpenFoam representation of N-S equation where momentum sink is represented by BodyForce, which is computed with different approaches as explained earlier.

fvVectorMatrix UEqn

(

   fvm::ddt(U) + fvm::div(phi, U) + turbulence->divDevReff(U)-fvc::grad(p)-BodyForce)   Equation 18
)

In AD, the major input to the model are thrust/power curve, tip and hub radius, wind direction and location of the wind turbine. In Simple actuator line model, the input parameters are turbine location, airfoil aerodynamic data, hub and tip radius, base location, turbine height, rotational speed and direction. The major outputs we get are the forces, torque, power etc. on each turbine and total power output of the wind farms. The advanced AL model is derived from the SOWFA code [11;12], the input and output are same as SOWFA code

A new turbulence model VLES has been implemented in OpenFoam. To implement VLES model existing k-epsilon library was modified by adding a filter function from Large Eddy Simulation library.

6. Validation-1: Validation of a single turbine

The first validation was done by performing the CFD simulation of a single wind turbine. In this study CFD simulation of a single siemens wind turbine 2.3 MW have been performed. The UPWARDS.ASM requires detailed description of wind turbine which includes aerofoil properties of wind turbine blades, control system, nacelle, and tower data. SWT-2.3 is a propriety of Siemens wind turbine and difficult to obtain the wind turbine data and to overcome this challenge, NREL has developed a generic 2.3MW wind turbine hereafter referred as NREL 2.3MW wind turbine. The NREL 2.3MW has been designed in a such way that the performance of this turbine (power and thrust of wind as a function of incoming velocity) matches well with the SWT 2.3MW. The NREL 2.3MW wind turbine is a conventional three-blade upwind variable-speed variable-blade pitch-

controlled turbine. Its rotor diameter is about 93 m and the hub height is 63 m. The rated wind speed is 11.4 m/s. The rated rotor speed is 12.1 rpm and the rated power is 2.3 MW.

The UPWARD.ASM model have been verified by performing a CFD simulations of a single NREL 2.3-MW wind turbine. CFD simulation requires a computational domain consisting of a single turbine with appropriate volume mesh and boundary conditions. Total five simulations at different speeds have been carried out and these wind speeds are set as 6 m/s, 7 m/s, 8 m/s, 9 m/s and 10 m/s, respectively. The wind turbine is placed in a domain of 1800 m x 800 m x 300 m as shown in Figure **2** .
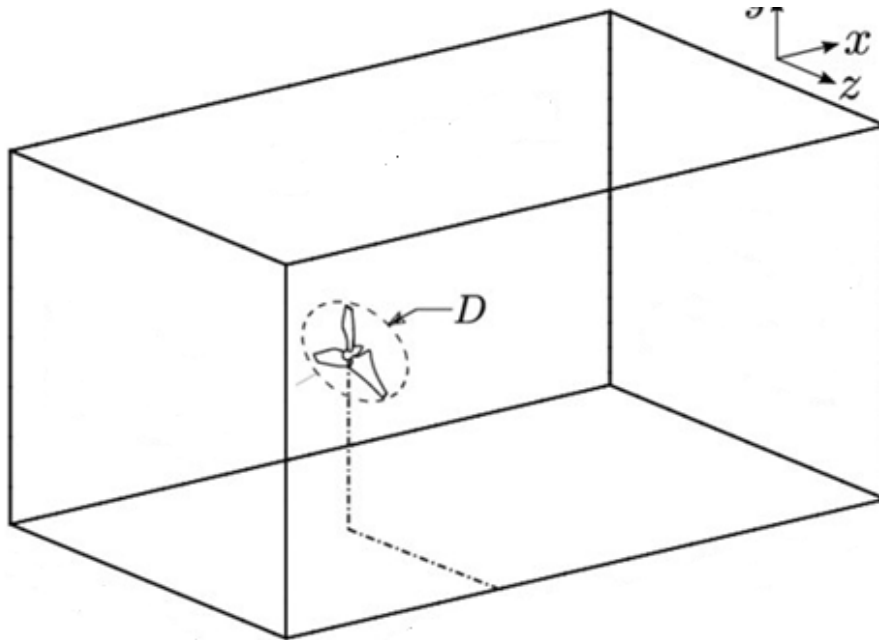

Figure 2: Computational domain used for NREL 2.3 MW wind turbine

Mesh is generated by blockMesh and snappyHexMesh in OpenFOAM. In the BlockMesh, initial mesh 150x120x60 was selected. Then the mesh around the wind turbine was refined using snappyHexMesh. The final mesh used in the simulations are shown in Figure. The inflow and outflow boundary conditions of velocity (U) are set by the fixedValue and inletOutlet, respectively, and zeroGradient and fixedValue are used correspondingly for the pressure (p). All other boundaries are defined as the slip boundary. The Reynolds-averaged Navier-Stokes (RANS) equations using the VLES turbulence model are considered in this model. Besides, the time-step size is set corresponding to a blade rotation of 1 degree and the data is saved every five-time steps. To obtain a relatively stable state, the simulation is calculated for 20 revolutions of the wind turbine. The Glauert model is chosen as the tip loss model. The results obtain using UPWARD.ASM is shown in the Figure **3**. The rotor power estimated at different wind speed is compared with the NREL data and the comparison is quite satisfactory. This validation was needed to ensure the model consistencies and to ensure that the input-output behaviour of model is in align with the other literature data.
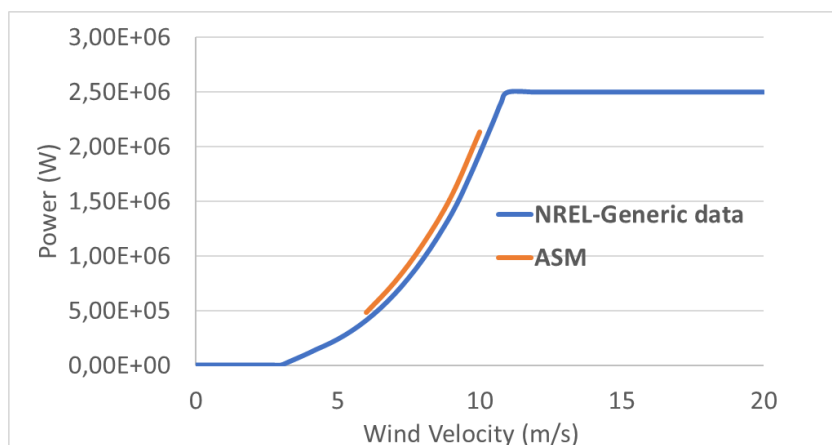

Figure 3: The power of the NREL 2.3MW wind turbine as a function of wind velocity

7. Validation-2: Lillgrund validation

After validating UPWARD.ASM for a single turbine, the objective was to verify with Lillgrund wind farms as mentioned in the Task 2.4. The simulated wind farm is Lillgrund offshore wind farm [29] operated by Vattenfall Vindkraft AB. Lillgrund is located in the Öresund, a body of water between Copenhagen, Denmark and Malmö, Sweden. Lillgrund offshore wind farm contain 48 Siemens SWT-2.3-93 three-bladed, upwind, horizontal-axis turbines [30] each with a rated power production of 2.3 MW, a rotor diameter of 93 m, and a rotor hub height of 65 m. Figure **4** show the plan view of the distribution of the wind turbine in the farm. The position of wind turbine is given in report from Jeppersson et al [29]. In our modelling the case set up was taken from SOWFA [30,31]. For ease on applying the boundary condition the computational domain was rotated along the wind direction as shown in Figure **4**
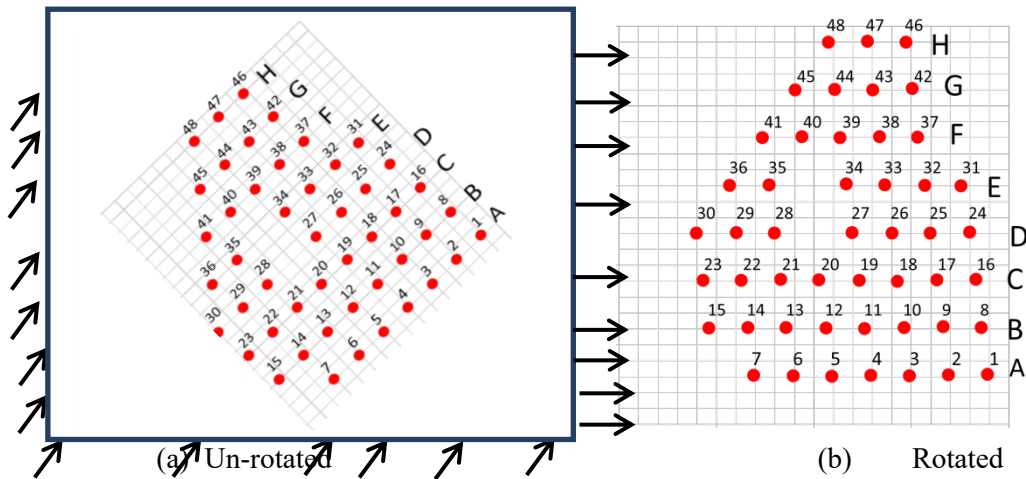

Figure 4: The plan view of the distribution of the wind turbine in the farm

Modelling of a wind park for a different wind direction is challenging task due to the fact that the yaw position of wind turbines changes with wind direction. In the present simulation, the computational domain is rotated to align with wind direction.

8.1 Computation Domain and Boundary condition

The computation domain used for the study is 5000 x 5000 x 400 m in axial, lateral and vertical direction respectively. Meshes are generated by blockMesh and snappyHexMesh in OpenFOAM. In the BlockMesh initial mesh 150x150x76 was selected and the corresponding 3D mesh is shown in Figure 5.
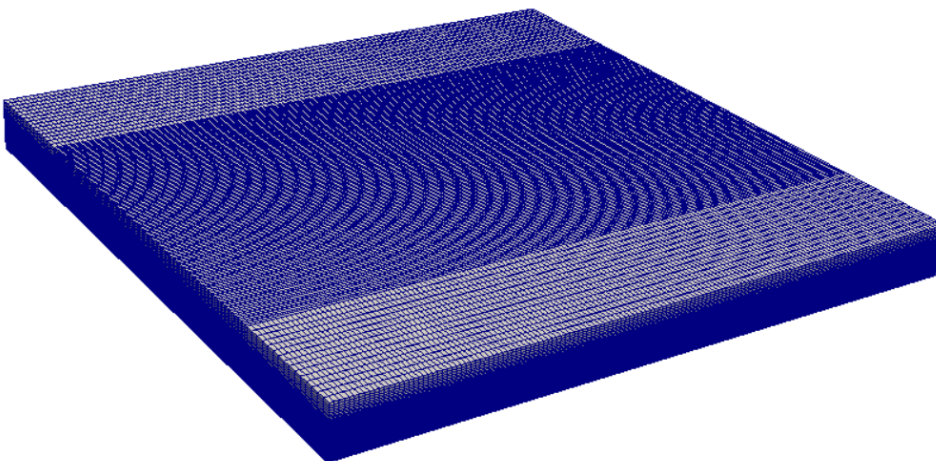

Figure 5: Three-dimensional grid of the computational domain

The mesh near to the wind turbine was refined using snappyHexMesh (see Figure 6). The total number of mesh points in these simulations were around 5 million meshes. The wind-wave interaction plays major role while modelling the offshore wind turbines. The sea surface waves are not modelled explicitly. Water surface is assumed as a flat surface without any roughness. A no-slip boundary condition is used on the bottom water surface. On the sides and top surface of computational domain free slip boundary condition is applied. At exit of the computational domain outlet boundary condition is used.
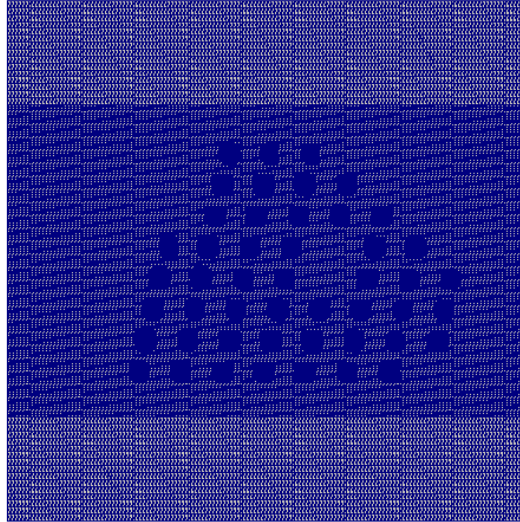

Figure 6: The grid in the turbine hub plane

One of the targets of this study was to evaluate the model by comparing the power production of the wind turbine. Our simulations are compared to the production data (presented by Dahlberg [32]) and LES simulation data (SOWFA solver [31]). Figure 7-Figure 12 show the power produced by each turbine normalized by the power of the corresponding of the first turbine of the row. The power prediction with UPWARDS.ASM is underpredicted compare to the SOWFA data specially for the second turbine. The reasons for this discrepancy was the choice of turbulence model and the mesh size. The current simulations were performed using 5 million cells on 12 processors compare to the SOWFA simulations in which 300 million cells on 4200 processors were used. In addition to this, the current simulations were performed using k-epsilon model which underpredicts the turbulence dissipation leading to the reduced wake mixing. We expected to see improvements in the result by using a fine mesh and also VLES turbulence model. However, these simulations are computationally demanding and are not performed yet, but these simulations will be repeated, and the results will be presented in a Journal. The UPWARDS.ASM is able to predict the effect of turbine distance on the velocity deficit and hence on power production as shown in Figure 11 and Figure 12.   The distance between turbine 27 and 28 in row E and 34 and 35 in row F is 6.6D compared to the 3.3D distance between next two turbines.
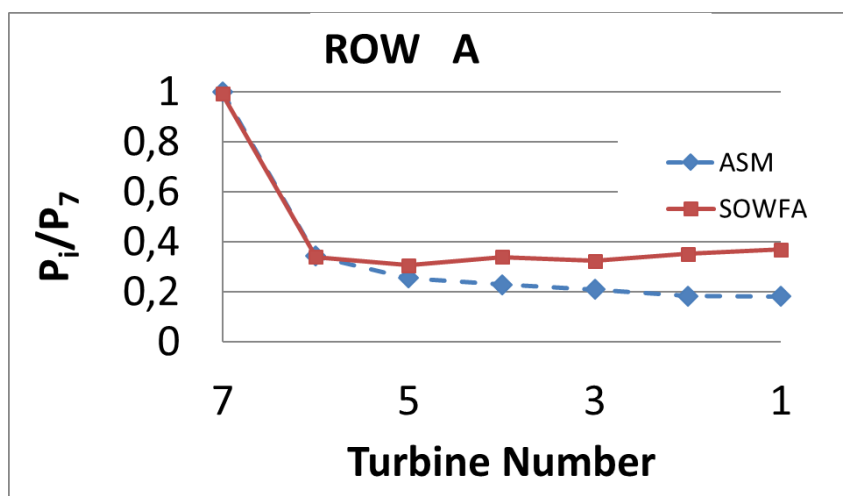

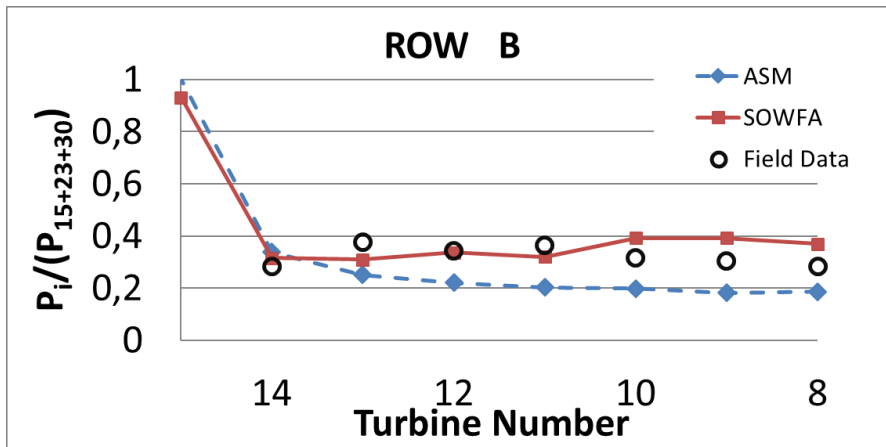**Figure 7 Normalized power of the wind turbines in row A for 221 wind direction**

Figure 8 Normalized power of the wind turbines in row B for 221 wind direction
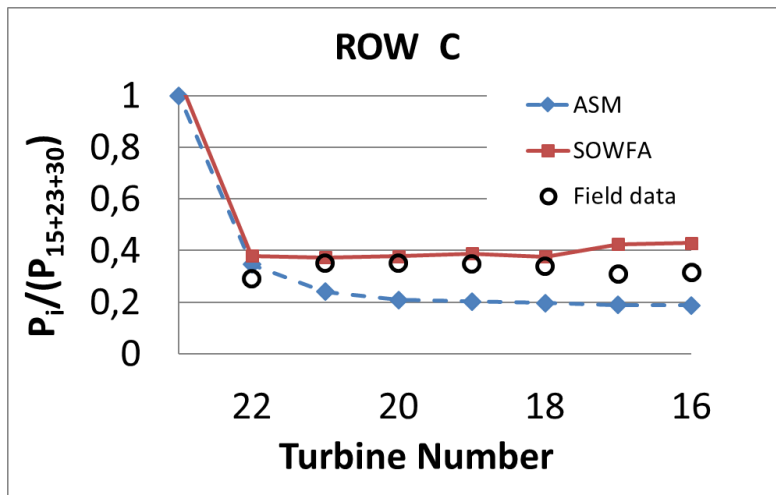

Figure 9 Normalized power of the wind turbines in row C for 221 wind direction
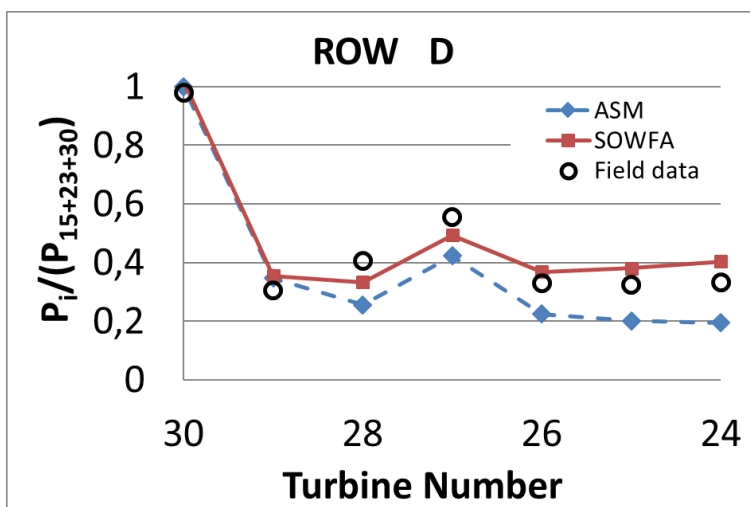

Figure 10 Normalized power of the wind turbines in row D for 221 wind direction
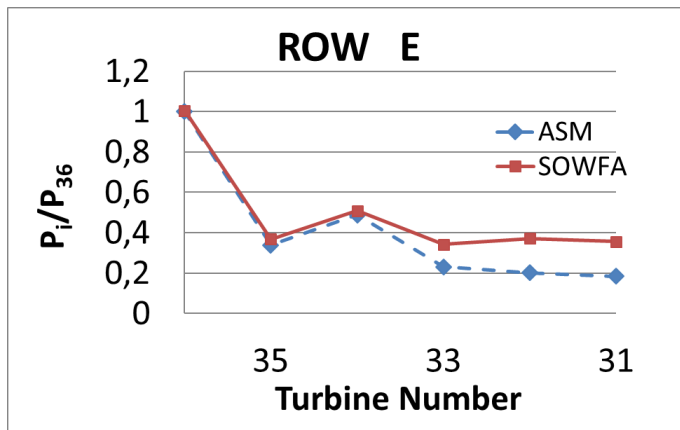
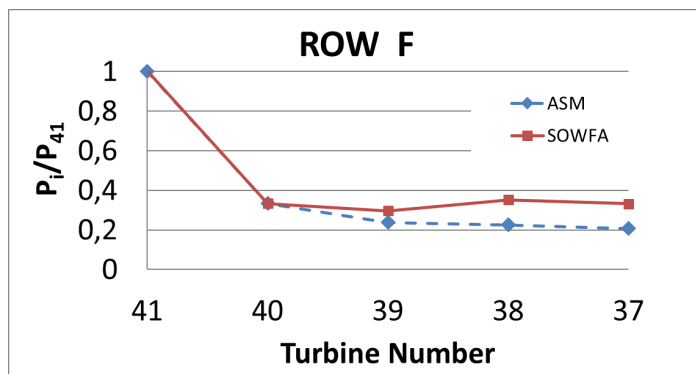Figure 11 Normalized power of the wind turbines in row E for 221 wind direction

Figure 12 Normalized power of the wind turbines in row F for 221 wind direction

8. Wind turbine simulations using VLES model

The purpose this study is to ensure the implemented VLES model works as expected. This verification study was performed by rerunning the single 2.3MW NREL wind turbine simulations using VLES model. The domain size, meshes, and boundary conditions are similar to the case as described in the section 6. Here the simulations were performed at 6, 7, 8, and 10 m/s. The power of the 2.3MW wind turbine is compared with NREL data and shown in the Figure **13**.
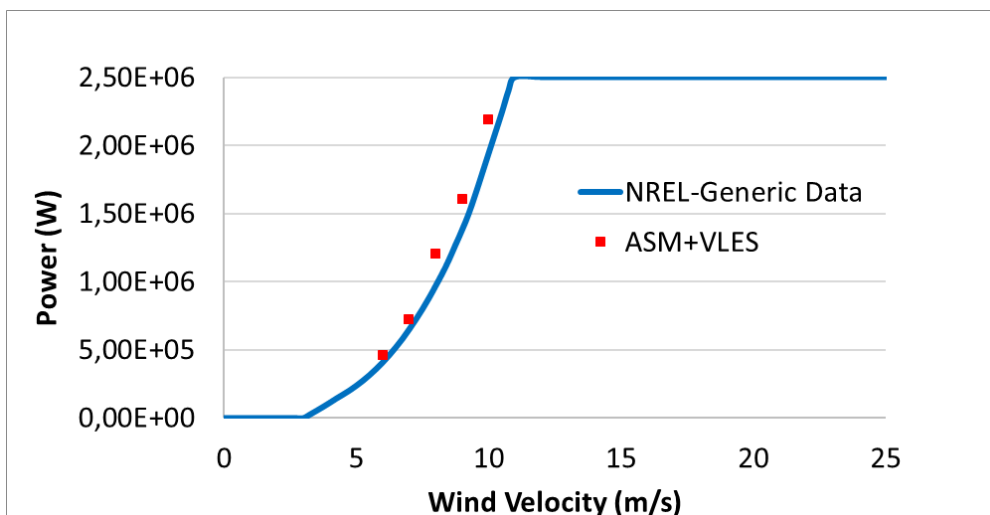

Figure 13: The power of the NREL 2.3MW wind turbine as a function of wind velocity

9. Conclusions

The existing actuator line model has some challenges and to overcome those challenges an improved ALM approach, Actuator Surface Models (ASM) for turbine blades, which take into account more geometrical details was implemented in OpenFom. The new OpenFoam application called "UPWARDS.ASM" has been created. The effect tower and nacelle is also included in the wind farm simulations. The model was verified and validated with available literature data and preliminary results are presented here. Filter-based turbulence model developed by SINTEF have been implemented and tested. The model seems to be working as expected but there is some discrepancy in power estimation when more than two turbines are placed in a row.

10. References

1. Yang, X.; Sotiropoulos, F. A new class of actuator surface models for wind turbines. *ArXiv170202108 Phys.* **2017**.
2. Linton, D.; Barakos, G.; Widjaja, R.; Thornber, B. A New Actuator Surface Model with Improved Wake Model for CFD Simulations of Rotorcraft. 10.
3. Kim, T. Improved actuator surface method for wind turbine application. *Renew. Energy* **2015**, 11.
4. Dobrev, I.; Massouh, F.; Rapin, M. Actuator surface hybrid model. *J. Phys. Conf. Ser.* **2007**, *75*, 012019.
5. Vermeer, L.J.; Sørensen, J.N.; Crespo, A. Wind turbine wake aerodynamics. *Prog. Aerosp. Sci.* **2003**, *39*, 467–510.
6. Ainslie, J.F. Calculating the flowfield in the wake of wind turbines. *J. Wind Eng. Ind. Aerodyn.* **1988**, *27*, 213–224.
7. Anderson, M. Simplified Solution to the Eddy-Viscosity Wake Model. 7.
8. Katic., I.; Höjstrup, O.; Jensen, N.O. A SIMPLE MODEL FOR CLUSTER EFFICIENCY.; Rome - Italy., 1986.
9. González-Longatt, F.; Wall, P.; Terzija, V. Wake effect in wind farm performance: Steady-state and dynamic behavior. *Renew. Energy* **2012**, *39*, 329–338.
10. S. Lissaman, P.B. Energy Effectiveness of Arbitrary Arrays of Wind Turbines. *J. Energy* **1979**, *3*, 323–328.
11. Voutsinas, S.G.; Rados, K.G.; Zervos, A. The effect of the non-uniformity of the wind velocity field in the optimal design of wind parks'.; Madrid, 1990.
12. *Advancement of Jensen (Park) wake model*; European Wind Energy Association, Ed.; Curran: Red Hook, NY, 2014; ISBN 978-1-63266-314-6.
13. Sørensen, J.N.; Myken, A. Unsteady actuator disc model for horizontal axis wind turbines. *J. Wind Eng. Ind. Aerodyn.* **1992**, *39*, 139–149.
14. Sørensen, J.N.; Kock, C.W. A model for unsteady rotor aerodynamics. *J. Wind Eng. Ind. Aerodyn.* **1995**, *58*, 259–275.
15. Sørensen, J.N.; Shen, W.Z.; Munduate, X. Analysis of wake states by a full-field actuator disc model. *Wind Energy* **1998**, *1*, 73–88.
16. Mikkelsen, R.; Technical University of Denmark; Department of Mechanical Engineering, F.M.; MEK Actuator disc methods applied to wind turbines, Lyngby, 2003.
17. Réthoré, P.-E.; van der Laan, P.; Troldborg, N.; Zahle, F.; Sørensen, N.N. Verification and validation of an actuator disc model: Verification and validation of an actuator disc model. *Wind Energy* **2014**, *17*, 919–937.
18. Sorensen, J.N.; Shen, W.Z. Numerical Modeling of Wind Turbine Wakes. *J. Fluids Eng.* **2002**, *124*, 393.
19. Aitken, M.L.; Kosović, B.; Mirocha, J.D.; Lundquist, J.K. Large eddy simulation of wind turbine wake dynamics in the stable boundary layer using the Weather Research and Forecasting Model. *J. Renew. Sustain. Energy* **2014**, *6*, 033137.
20. Churchfield, M.J.; Lee, S.; Schmitz, S.; Wang, Z. Modeling Wind Turbine Tower and Nacelle Effects within an Actuator Line Model. In Proceedings of the 33rd Wind Energy Symposium; American Institute of Aeronautics and Astronautics: Kissimmee, Florida, 2015.
21. Wu, Y.-T.; Porté-Agel, F. Large-Eddy Simulation of Wind-Turbine Wakes: Evaluation of Turbine Parametrisations. *Bound.-Layer Meteorol.* **2011**, *138*, 345–366.
22. Menter, F.R. Two-equation eddy-viscosity turbulence models for engineering applications. *AIAA J.* **1994**, *32*, 1598–1605.

23. El Kasmi, A.; Masson, C. An extended model for turbulent flow through horizontal-axis wind turbines. *J. Wind Eng. Ind. Aerodyn.* **2008**, *96*, 103–122.

24. Johansen, S.T.; Wu, J.; Shyy, W. Filter-based unsteady RANS computations. *Int. J. Heat Fluid Flow* **2004**, *25*, 10–21.

25. Olsen, J.E.; Skjetne, P.; Johansen, S.T. VLES turbulence model for an Eulerian–Lagrangian modeling concept for bubble plumes. *Appl. Math. Model.* **2017**, *44*, 61–71.

26. Labois, M.; Lakehal, D. Very-Large Eddy Simulation (V-LES) of the flow across a tube bundle. *Nucl. Eng. Des.* **2011**, *241*, 2075–2085.

27. Panjwani, B.; Olsen, J.E. Design and modelling of dust capturing system in thermally stratified flowing conditions. *Build. Environ.* **2020**, *171*, 106607.

28. Launder, B.E.; Spalding, D.B. The numerical computation of turbulent flows. *Comput. Methods Appl. Mech. Eng.* **1974**, *3*, 269–289.

29. Jeppsson, J.; Larsen, P.E.; and Larsson, � *Technical Description Lillgrund Wind Power Plant,Vattenfall Vindkraft AB, 2_1 LG Pilot Report, Sept. 2008*; 2008;

30. Churchfield, M.J.; Lee, S.; Michalakes, J.; Moriarty, P.J. A numerical study of the effects of atmospheric and wake turbulence on wind turbine dynamics. *J. Turbul.* **2012**, *13*, N14.

31. Churchfield, M.; Lee, S.; Moriarty, P.; Martinez, L.; Leonardi, S.; Vijayakumar, G.; Brasseur, J. A large-eddy simulation of wind-plant aerodynamics. In Proceedings of the 50th AIAA Aerospace Sciences Meeting including the New Horizons Forum and Aerospace Exposition; 2012; p. 537.

32. Dahlberg, J.� *Assessment of the Lillgrund Wind Farm: Power Performance Wake Effects,Vattenfall Vindkraft AB, 6_1 LG Pilot Report*; 2009;